Chapter 11

Characterising contrast agents for magnetic resonance imaging

Belorizky E. [a] and Fries P.H. [b]

[a] *Interdisciplinary Laboratory of Physics, Grenoble Alpes University, Grenoble.*

[b] *Ionic Recognition and Coordination Chemistry, Inorganic and Biological Chemistry, UMR-E3, Grenoble Alpes University, Grenoble*.

11.1 - Introduction

Techniques for medical diagnosis, and more generally, preclinical research – used to non-invasively observe the inside of living organisms – have developed considerably over the last few decades. The most commonly used are based on X-rays [Ledley *et al*., 1974], ultrasound [Correas *et al.*, 2009] or nuclear magnetic resonance of water protons from tissues, i.e., observation of how these nuclei, placed in a fixed external magnetic field, respond to excitation created by an oscillating magnetic field [Canet *et al.,* 2002]. This phenomenon constitutes the basis of Magnetic Resonance Imaging (MRI) [Mansfield and Pykett, 1978; Merbach and Toth, 2001; Callaghan, 2003]. The submillimetre resolution of this method is remarkable, but it lacks the requisite *sensitivity* for some examinations. For example, it cannot detect small anatomical anomalies such as burgeoning tumours or low-concentration molecular species characteristic of diseases such as those forming fatty deposits (atheromatous plaques) in the arteries. The contrast of images of tissues or anomalies can be improved by injecting biocompatible paramagnetic species, known as *contrast agents* [Bertini *et al.*, 2001]. These agents are often gadolinium Gd^{3+} complexes. The physical mechanisms explaining how they improve contrast are difficult to

P. Bertrand, *Electron Paramagnetic Resonance Spectroscopy*,
https://doi.org/10.1007/978-3-030-39668-8_11

model as they involve multiple phenomena, such as translational Brownian motion of the water molecules, rotational Brownian motion of the complexes, and random evolution of the quantum states of the electronic spin of the Gd^{3+} causing its relaxation. EPR of Gd^{3+} complexes can effectively contribute to characterising these phenomena.

In this chapter, we briefly present the principle by which MRI images are constructed, in particular those based on spatial variations of local relaxation times for water protons. The role of contrast agents is explained by underlining the specific advantages of Gd^{3+} complexes. Then, the mechanisms leading to relaxation of the protons contained in the tissue water are analysed and classed as a function of the properties through which the water molecules associate with complexes in solution. We show how the electronic relaxation of Gd^{3+} affects the performance of contrast agents, and the key contribution of EPR to quantifying this relaxation. We propose a theoretical formalism through which to simulate EPR spectra and thus determine the electronic relaxation. This formalism is applied to a few representative Gd^{3+} complexes in aqueous solution and we assess their usefulness as contrast agents. Finally, we present a few images obtained using some of these complexes.

11.2 - MRI methods

11.2.1 - General principle

As indicated, biomedical MRI is a non-invasive technique based on observation of the Nuclear Magnetic Resonance (NMR) signal produced by the protons from the hydrogen atoms in water [Canet, 1996; Abragam, 1983]. Indeed, as water makes up around 70 % of the human body, ^1H protons are highly abundant and supply a good NMR signal. The intensity of the signal observed depends on the water concentration which is relatively constant in soft tissues, but is mostly influenced by the relaxation times for nuclear spins, which characterise the speed of return to equilibrium of the magnetic moments of the protons following excitation. More precisely, by applying a series of radiofrequency radiation pulses and magnetic field gradients in the three spatial directions, a region of the organism can be divided into juxtaposed elementary volumes (voxels) producing distinct NMR signals which are a function of the density ρ of protons and the longitudinal T_1 and transverse T_2 relaxation times specific to each voxel [Merbach and Toth, 2001; Callaghan, 2003]. The type of

measurement performed reveals differences in the values of ρ, T_1 or T_2 between different voxels. These differences can be coloured in greyscale, to produce images that are weighted in proton density, T_1 or T_2. For example, lesions in tissues or tumours can be observed thanks to differences in the relaxation times for water between the healthy and affected areas.

In general, the T_1 and T_2 values vary as follows [Abragam, 1983]:

- T_1 is shorter in common solvents like water (a few seconds) than in viscous liquids and solids (several minutes or more). Indeed, rapid, large-amplitude molecular movement in non-viscous liquids promote transitions between Zeeman levels of protons causing faster T_1 relaxation than their slow, weak-amplitude equivalents in solids.
- T_2 is longer in common solvents than in viscous liquids as variations in the local field, which determine the T_2 relaxation, are caused by faster molecular movements and are thus more rapidly averaged to zero. This phenomenon is known as motional narrowing.
- T_1 is always greater than or equal to T_2. T_1 and T_2 have similar values in pure water and non-viscous liquids, but the differences between them can be considerable in solids (T_1 a few hours, T_2 a few ms).

In biological tissues, T_1 increases as the field B increases, whereas T_2 is relatively independent of the field [Abragam, 1983; Canet, 1996]. These relaxation times depend on the physico-chemical organisation of the water in the region of the organism observed. Radiologists exploit spatial variations in the values of T_1 or T_2 to produce anatomical images and use abnormal variations of these times to detect lesions and diseased areas in the tissues. In Table 11.1, we have indicated the values of T_1 and T_2 for some healthy tissues *in vivo* at 37 °C and for distilled water at 20 °C, in a 1.5-T field.

Table 11.1 - Relaxation times for protons in some healthy tissues *in vivo* and for water in a 1.5-tesla magnetic field.

Tissue	T_1 [ms]	T_2 [ms]
Adipose tissue [a]	282	111
Muscle [a]	749	43
Liver [a]	594	61
Cortex [b]	1304	93
White matter [b]	660	76
Distilled water [c]	2780	1400

[a] [Tadamura *et al.,* 1997], [b] [Vymazal *et al.,* 1999], [c] [Kiricuta and Simplaceanu, 1975].

In general, at the magnetic fields commonly used in MRI ($B \leq 1.5$ T), the relaxation times for protons in well-hydrated tissues, which are thus of low viscosity, increase with the water content as water is the most mobile species [Kiricuta and Simplaceanu, 1975] (also see sections 11.3.2 and 11.3.3). Schematically, in the case of an acute disorder, the proton density and T_1 and T_2 times vary in the same direction for a given tissue. Indeed, in most cases lesions are associated with inflammation and oedema characterised by infiltration of water into the affected tissue. The opposite occurs in scar tissue.

For many MRI sequences with appropriately selected parameters, the signal intensity for a voxel increases with the longitudinal relaxation rate $R_1 = 1/T_1$, but decreases with the transversal relaxation rate $R_2 = 1/T_2$ [Merbach and Toth, 2001; Callaghan, 2003].

11.2.2 - Role of contrast agents in MRI

The contrast agents considered here are chemical complexes which modify the NMR signal for the voxels where they are located, by increasing the relaxation rates $R_1 = 1/T_1$ and $R_2 = 1/T_2$ for water protons. The increases are generally proportional to the local concentration of relaxing agents, which depends on the properties of the different tissues. Thus, differences in the proton relaxation enhancement reflect biological differences such as the presence of tumour tissue. More significant differences generally produce better image contrast enhancement. The most frequently used contrast agents are complexes or chelates of paramagnetic metal ions, i.e., constructs composed of organic

molecules (ligands) sequestering one or sometimes several of these ions. Less frequently, super-paramagnetic nanoparticles are also used, for example iron oxide particles composed of several thousand magnetic ions, with their individual magnetic moments aligned to produce a very high resultant paramagnetic moment [Merbach and Toth, 2001].

Here, we will only discuss complexes of a single metal ion bearing a high magnetic moment, capable of creating a large-amplitude fluctuating dipolar field in its surroundings, which notably accelerates proton relaxation. The appropriate ions belong either to the first transition series (manganese, iron), or to the lanthanide series (gadolinium, dysprosium), which have a 3*d* and a 4*f* incomplete atomic subshell, respectively. The contrast agents currently commercialised generally contain Gd^{3+} as it provides the best contrast enhancement for T_1-weighted images.

11.3 - Effect of a Gd^{3+} complex on relaxation of water protons

11.3.1 - General notions

Consider an aqueous solution of GdL complexes, where Gd is the paramagnetic ion Gd^{3+} and L is a multidentate ligand. Remember that the Gd^{3+} ion has a half-filled $4f^7$ subshell and that its ground term $^8S_{7/2}$ is characterised by a total orbital momentum $L = 0$, a total spin $S = 7/2$ and a Landé g factor close to that of the electron [Volume 1, section 8.1.1]. This ion has two isotopes with nuclear spin $I = 3/2$, but the hyperfine structure is not involved here due to the broad width of the EPR lines [Borel *et al.,* 2006]. The longitudinal relaxation rate $R_1 = 1/T_1$ for water protons in this solution is the sum of the diamagnetic contribution $R_{1,d}$ obtained in the absence of complexes and of the $R_{1,p}$ contribution due to paramagnetic complexes:

$$R_1 = R_{1,d} + R_{1,p} \qquad [11.1]$$

This relation only applies with dilute solutions such as those monitored by MRI. Experiments demonstrate, and the theory confirms (sections 11.3.2 and 11.3.3), that $R_{1,p}$, which represents the increase in the relaxation rate due to GdL complexes, is generally proportional to the molar concentration [GdL]. The *relaxivity* r_1 of these complexes is defined by the relation

$$R_1 = R_{1,d} + r_1[\mathrm{GdL}] \qquad [11.2]$$

i.e., by the slope of the line giving R_1 as a function of [GdL] expressed in mM (mmol L^{-1}).

Relaxivity is therefore expressed in s^{-1} mM^{-1}. Hereafter, we describe the different elements contributing to it.

Paramagnetic relaxation of the spin I of a water proton is due to fluctuations of its dipolar interactions with the magnetic moments of Gd^{3+} ions. In the point dipole approximation, in which the magnetic moment for each Gd^{3+} ion is considered to be localised at the centre of the ion [Yazyev and Helm, 2008], this interaction is described by the following Hamiltonian [Volume 1, section 7.2.4]:

$$\hat{H}_{dip} = \frac{\mu_0}{4\pi}\gamma_I\gamma_S\hbar^2\left[\mathbf{I}\cdot\mathbf{S} - 3(\mathbf{I}\cdot\mathbf{r})(\mathbf{S}\cdot\mathbf{r})\Big/r^2\right]\Big/r^3 \qquad [11.3]$$

where μ_0 is the permeability of a vacuum, γ_I, γ_S are, respectively, the magnetogyric ratios of the proton and Gd^{3+}, and $\mathbf{r}$ is the vector linking the Gd^{3+} ion to the proton. Two relaxation mechanisms are generally distinguished: the inner sphere and the outer sphere mechanisms.

Inner sphere mechanism. As $\hat{H}_{dip}$ increases as $1/r^3$ when the distance r decreases, the protons in the water molecules close to the Gd^{3+} ions have a very large instantaneous relaxation rate. Thus, the molecular movements resulting in transient coordination of the water molecules to the metal ions and thus bringing the water protons close to these ions, play an important role in transmitting the effect of paramagnetic relaxation to the whole of the solvent. The water molecules bound (coordinated) to the metal form the first coordination sphere or *Inner-Sphere* (IS). These inner sphere water molecules, in which the protons have an extremely high *intrinsic intramolecular relaxation rate* $R_{1m} \equiv 1/T_{1m}$ ($T_{1m} \cong$ a few μs), then exchange with solvent protons such that, in turn, all the solvent molecules, when they come into contact with Gd^{3+} undergo the intrinsic inner sphere paramagnetic relaxation. This overall mechanism is described as the inner sphere contribution R_1^{IS} to $R_{1,p}$ (figure 11.1).

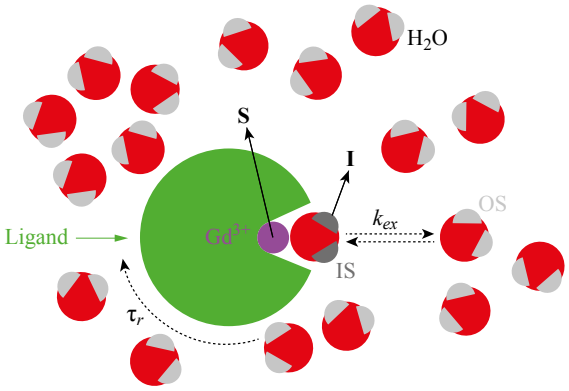

Figure 11.1 - Schematic representation of a Gd^{3+} complex (ion green, ligand red) to which an inner sphere (IS) water molecule is bound. This water molecule is surrounded by so-called outer sphere (OS) free water molecules from the solvent. k_{ex} is the rate constant for exchange between inner sphere water molecules and free molecules. It is linked to their lifetime τ_m by $k_{ex} = 1/\tau_m$ (see the text). τ_r is the rotational correlation time for the complex which is particularly involved in the expression for T_{1m} (equation [11.8]).

Outer sphere mechanism. For durations approximately equal to the lifetime τ_m of an inner sphere water molecule, no chemical exchange occurs but protons in the free water molecules experience another paramagnetic relaxation effect due to their relative *intermolecular translational diffusion* motion with respect to the Gd^{3+} ions. This motion is known as *Outer Sphere* OS motion and this effect produces the outer sphere contribution R_1^{OS} to $R_{1,p}$. We have thus defined the inner and outer sphere contributions to $R_{1,p}$ as a function of the intra- and intermolecular nature of the fluctuations in the dipolar interaction over times with an order of magnitude of around τ_m. The total increase in the relaxation rate for the protons due to GdL complexes can therefore be written

$$R_{1,p} = R_1^{IS} + R_1^{OS} \qquad [11.4]$$

and the total relaxivity is given by

$$r_1 = r_1^{IS} + r_1^{OS} \qquad [11.5]$$

With some complexes, another type of fluctuation of the dipolar interaction – intramolecular fluctuation – gives a "second sphere" contribution. This contribution is due to labile water molecules located close to the metal ion, which are not directly coordinated to the complex, as in the case of the inner sphere mechanism, but by *hydrogen bonding with the ligand*. The second sphere

contribution $R_{1,p}^{2S}$ can be described as the inner sphere contribution. However, it is often negligible, or its effects are (incorrectly) taken into account in the outer sphere term [Aimé *et al.*, 2005; Bonnet *et al.*, 2010].

The Gd^{3+}-based contrast agents commonly used in medical MRI have been known since the mid-1980s. They produce comparable inner and outer sphere relaxivities, of around 1 to 2 s^{-1} mM^{-1} at the field generally used in imaging, 1 to 3 T [Powell *et al.* 1996]. However, chemists progressively obtained much larger inner sphere relaxivity values r_1^{IS} by synthesising a new generation of contrast agents developed according to the prescriptions of theoretical models (sections 11.3.2 and 11.9) [Aimé *et al.* 2005; Caravan, 2009; De Leon-Rodriguez *et al.* 2009]. Optimisation of the outer sphere contribution r_1^{OS}, in contrast, is much more difficult to conceive. We will now analyse the factors which determine the two main types of relaxivity and produce simplified theoretical expressions for R_1^{IS} and R_1^{OS}.

11.3.2 - Inner sphere proton relaxivity

The inner sphere contribution to proton relaxation results from fluctuations in the intramolecular dipolar interaction of the protons of the water molecules coordinating Gd^{3+} and exchanges between these molecules and the water molecules in the solution. This is a two-site exchange problem; the first site, represented by the water molecules *bound* to the metal ion, is much less populated than the second, represented by the *free* water molecules. The experimental NMR signal is that of protons in free water. In complement 1 we show that the inner sphere relaxation rate is given by

$$R_1^{IS} = P_m \frac{1}{T_{1m} + \tau_m} \qquad [11.6]$$

where P_m is the molar fraction of bound protons, τ_m is the lifetime of an inner sphere water molecule, linked to the exchange rate constant k_{ex} (figure 11.1) by $\tau_m = 1 \,/\, k_{ex}$ and T_{1m} is the intrinsic longitudinal relaxation time for bound protons in the absence of exchange, i.e., in the situation where the water molecule would remain indefinitely coordinated to Gd^{3+}. The molar fraction P_m is linked to [GdL], the molar concentration of complexes, and to q, the number of water molecules bound to a Gd^{3+} ion (solvation number), by the relation

$$P_m = \frac{q[\mathrm{GdL}]}{55.5} \qquad [11.7]$$

For the Gd^{3+} complexes used as contrast agents, τ_m is typically around 10^{-7} to 10^{-6} s. In general, the main contribution to the relaxation rate $R_{1m} \equiv 1/T_{1m}$ is due to the modulation of the dipole-dipole interaction $\hat{H}_{dip}$ (equation [11.3]) by the reorientational Brownian motion of the $\mathbf{r}_{GdH}$ vector with constant magnitude, linking the centre of the Gd^{3+} ion to the bound water proton considered. In the absence of electronic relaxation of the paramagnetic ion, this relaxation rate is given by the simplified Solomon-Bloembergen-Morgan (SBM) equation, which is valid with the fields used in MRI [Merbach and Toth, 2001]:

$$R_{1m} = \frac{1}{T_{1m}} = \left(\frac{\mu_0}{4\pi}\right)^2 \frac{2}{5}\left(\frac{\gamma_I^2 g^2 \beta^2}{r_{GdH}^6}\right) S(S+1)\frac{\tau_r}{1+\omega_0^2\tau_r^2} \qquad [11.8]$$

where g is the Landé factor for the Gd^{3+} ion of spin $S = 7/2$, β is the Bohr magneton ($\gamma_S \hbar \mathbf{S} = -g\beta\mathbf{S}$), ω_0 is the resonance angular frequency for the proton, and τ_r is the rotational correlation time for the complex. For a spherical complex of radius a, this time is approximately given by the Stokes rotational diffusion formula

$$\tau_r = \frac{4\pi a^3 \eta_{mic}^r}{3k_B T} \qquad [11.9]$$

where T is the temperature. The rotational microviscosity η_{mic}^r of the solution [Gierer and Wirtz, 1953] can differ significantly from the experimentally measured macroscopic viscosity because of the granular structure (finite size) of the molecules. Qualitatively, τ_r represents the mean time required for the complex to perform a rotation of 1 radian due to the effect of collisions with solvent molecules. For the complexes considered, τ_r is around 10^{-10} s at room temperature, but it increases to 10^{-8} s for bulkier complexes.

Equation [11.8] shows that a first advantage of the Gd^{3+} ion is the high value $S = 7/2$ of its electronic spin, which can result in high values of R_{1m} thanks to the $S(S+1)$ factor. The distance r_{GdH} varies little between complexes, being consistently around 0.31 ± 0.01 nm [Caravan, 2009]. For typical values $B \leq 1.5$ T, $\tau_r = 10^{-9}$ s, equation [11.8] gives a very high value, practically independent of B, $R_{1m} \cong 1.5 \times 10^6\ s^{-1}$, or $T_{1m} \cong 0.7\ \mu s$. In an imager with a given magnetic field B where the resonance frequency ω_0 of the protons is fixed, R_1^{IS} can be increased by optimising three parameters through chemical synthesis (equation [11.6]): the exchange rate $k_{ex} = 1/\tau_m$, the solvation number q (equation [11.7]), and the correlation time τ_r (equation [11.8]).

11.3.3 - Outer sphere proton relaxivity

The contribution of outer sphere proton relaxivity is the result of fluctuations in the magnetic dipolar interaction $\hat{H}_{dip}$ between the magnetic moment $\gamma_S \hbar \mathbf{S}$ for each complexed Gd^{3+} ion and $\gamma_I \hbar \mathbf{I}$, the magnetic dipole for each proton in the water molecules which are free relative to the complex, i.e., undergoing random relative translational diffusion motion. The corresponding relaxation rate R_1^{OS} can be determined by applying the Torrey [Torrey, 1953] and Solomon theory [Abragam, 1983; Solomon, 1955]:

$$R_1^{OS} = C[3j_2(\omega_I) + 7j_2(\omega_S)] \qquad [11.10]$$

where

$$C = \frac{32\pi}{405}\left(\frac{\mu_0}{4\pi}\right)^2 \gamma_I^2 g^2 \beta^2 S(S+1)\frac{\mathcal{N}_A[\mathrm{GdL}]}{bD} \qquad [11.11]$$

In these expressions, ω_I and ω_S are the resonance angular frequencies of the spins I and S. If we note $\mathbf{r}(r, \theta, \varphi)$ the vector linking the proton to the Gd^{3+} ion, the spectral density $j_2(\omega)$ is the Fourier cosine transform of the temporal dipolar correlation function $g_2(t)$ of the random function $r^{-3}Y_{20}(\theta, \varphi)$, where $Y_{20}(\theta,\varphi) \equiv \sqrt{5/(4\pi)}(3\cos^2\theta - 1)/2$ is a second order spherical harmonic. In equation [11.11], $\mathcal{N}_A[\mathrm{GdL}]$ is the number of complexes per unit of volume, where $\mathcal{N}_A$ is Avogadro's number and [GdL] is the concentration of Gd^{3+} ions in mM; b is the minimal approach distance between the interacting magnetic moments, and $D = D_I + D_S$ is the relative diffusion coefficient of a water molecule and a complex, equal to the sum of the coefficients for water self-diffusion D_I and diffusion of the complex D_S. The expression for $j_2(\omega)$ is difficult to calculate for the most general intermolecular motion which results from translational and rotational movements of the water and the complex as well as any changes in complex conformation. However, $j_2(\omega)$ has a simple closed form expression in the following case:

- the water molecules and the complex are hard impenetrable spheres with centred magnetic moments,
- the free water molecules are uniformly distributed around the complex. This is a reasonable approximation [Ayant *et al.* 1975; Hwang and Freed, 1975]. In this case, we obtain:

$$j_2(\omega) = \mathrm{Re}\frac{1 + z/4}{1 + z + 4z^2/9 + z^3/9} \qquad [11.12]$$

Re designates the real part and $z = \sqrt{i\omega\tau_D}$, τ_D is a translational correlation time given by $\tau_D = b^2/D$, where b is the sum of the molecular radii for the two species. By order of magnitude, τ_D is the mean time necessary for a water molecule to cover the distance $b/2$. Typically, τ_D is around 10^{-10} s at room temperature. Equations [11.10] and [11.11] indicate that R_1^{OS} is proportional to $S(S+1)$ as R_{1m} (equation [11.8]), so that the high spin $S = 7/2$ of Gd^{3+} also favours high R_1^{OS} values. If we set $u \equiv \sqrt{2\omega\tau_D}$, expression [11.12] can be written in the form of a rational fraction with a real argument

$$j_2(\omega) = \frac{1 + 5u/8 + u^2/8}{1 + u + u^2/2 + u^3/6 + 4u^4/81 + u^5/81 + u^6/648} \quad [11.13]$$

The spectral density $j_2(\omega)$ is a decreasing function of ω which varies as $1-(3/8)\sqrt{2\omega\tau_D}$ at low frequencies ($\omega\tau_D \ll 1$) and as $(81/4)/(\omega\tau_D)^2$ at high frequencies ($\omega\tau_D \gg 1$).

It should be noted that the distinction between inner and outer sphere mechanisms implies τ_r, $\tau_D \ll \tau_m$. This inequality is generally verified.

11.3.4 - Influence of the electronic spin relaxation of Gd^{3+}

Expressions [11.6], [11.8], [11.10], [11.12], which give the paramagnetic relaxation rates, were obtained by assuming that the electronic relaxation times for the Gd^{3+} complex are infinitely long. In fact, electronic relaxation of the complex affects the inner and outer sphere relaxivity of the water protons [Bertini *et al.*, 2001; Kowalewski and Maler, 2006]. At the magnetic fields used in imaging ($B \geq 1$ T), the effects of electronic relaxation only depend on the longitudinal electronic relaxation time T_{1e} [Fries and Belorizky, 2007; Belorizky *et al.*, 2008; Bonnet *et al.*, 2008]:

- in the case of the inner sphere mechanism, expression [11.8] becomes:

$$R_{1m} = \frac{1}{T_{1m}} = \left(\frac{\mu_0}{4\pi}\right)^2 \frac{2}{5}\left(\frac{\gamma_I^2 g^2 \beta^2}{r_{GdH}^6}\right) S(S+1)\frac{\tau_1}{1+\omega_0^2\tau_1^2} \quad [11.14]$$

  the rotational correlation time τ_r is thus replaced by the *effective correlation time* τ_1 defined by:

$$\frac{1}{\tau_1} = \frac{1}{\tau_r} + \frac{1}{T_{1e}} \quad [11.15]$$

- in the case of the outer sphere mechanism, the z variable in equation [11.12] becomes $z = \sqrt{i\omega\tau_D + \tau_D/T_{1e}}$ [Bonnet *et al.*, 2008].

At this stage, it is already obvious that electronic relaxation of Gd^{3+} complexes affects their relaxivity. This direct effect is sufficient to justify devotion of a whole chapter to contrast agents in a book on EPR applications. However, we will see in sections 11.4.1 and 11.4.2 that interpretation of the electronic relaxation can also be used to determine the correlation time τ_r involved in the inner sphere process. Finally, its role is important when analysing the relaxation of ^{17}O nuclei of water, a process which can provide information on the exchange rate k_{ex} involved in equation [11.6] [Merbach and Toth, 2001]. It is therefore essential to determine the relaxation time T_{1e} for the Gd^{3+} complex.

With current technology, T_{1e} can be measured at X-band by longitudinal detection of EPR (LODEPR) technique based on observation of the response of the longitudinal magnetisation when the microwave power is modulated at a frequency of around $1/T_{1e}$ [Borel *et al.*, 2002]. The T_{1e} values measured for Gd^{3+} chelates in aqueous solution at room temperature are around 2 to 4 ns. But this very promising approach is currently limited to X-band magnetic fields (0.34 T) which are considerably lower than those used in imaging. For MRI applications, T_{1e} must be *calculated* using an appropriate model relying on analysis of conventional EPR spectra (see section 11.6).

Examination of equations [11.14] and [11.15] indicates why Gd^{3+} complexes are considerably better contrast agents than complexes of other lanthanides with a higher angular momentum J:

- Lanthanides Ln^{3+} with an atomic number greater than that of Gd^{3+} have a very short electronic relaxation time T_{1e}, of around 10^{-13} s [Bertini *et al.*, 2001; Vigouroux *et al.*, 1999; Fries and Belorizky, 2012]. When T_{1e} is much shorter than τ_r which is around 10^{-9} to 10^{-10} s, equation [11.15] shows that $\tau_1 \cong T_{1e} \ll \tau_r$. In these conditions, at the frequencies used in MRI, the following inequality holds $\omega_0\tau_1 \ll \omega_0\tau_r \leq 1$. The value of R_{1m} given by [11.14] is therefore proportional to T_{1e}, and is thus much smaller than that obtained when electronic relaxation is neglected, where it is essentially proportional to τ_r (equation [11.8]). The strong reduction in R_{1m} considerably increases T_{1m} which, according to equation [11.6], causes R_1^{IS} to be significantly reduced since contrast agents must satisfy the $\tau_m < T_{1m}$ criterion promoting an efficient inner sphere mechanism.

  Similarly, for the outer sphere contribution, a very short T_{1e} time such that $T_{1e} \ll \tau_D$ (τ_D is the translational correlation time) produces a much larger module of the variable z than in the absence of electronic relaxation. This

effect translates into a considerable decrease in the spectral density $j_2(\omega)$ and in the relaxation rate R_1^{OS}.

- ▹ In contrast, for Gd^{3+}, T_{1e} is around 10^{-8} s at the fields generally used in imaging. Therefore $T_{1e} \geq \tau_r$ et $T_{1e} \gg \tau_D$, such that attenuation of the relaxivity due to T_{1e}, although problematic, particularly for bulky complexes, is no longer insurmountable.

In summary, Ln^{3+} ions in which the 4*f* subshell is more than half full, with much shorter relaxation times T_{1e} than those for Gd^{3+}, produce a relaxivity much smaller than that provided by Gd^{3+} even if their angular momentum J is higher than the $S = 7/2$ spin of Gd^{3+}, as is the case for Dy^{3+} and Er^{3+} ($J = 15/2$), Tb^{3+} ($J = 6$) and Ho^{3+} ($J = 8$). The relative slowness of the electronic relaxation of Gd^{3+} is due to the fact that its ground term is characterised by $L = 0$. This term is therefore not affected to first order of perturbation theory by the random electrostatic field produced by the ligands which causes electronic relaxation [Volume 1, section 8.3.5]. In contrast, the ground states for the other Ln^{3+} ions, for example Tb^{3+}, Dy^{3+}, Ho^{3+} and Er^{3+} characterised by $L = 3, 5, 6, 6$, respectively, are directly affected by the dynamic effects of the ligand field [Merbach and Toth, 2001, chapter 8].

Below, we will model the relaxation mechanisms for Gd^{3+} complexes and provide simplified expressions for T_{1e} as a function of a restricted number of parameters, then we will show how these parameters can be determined from simulated EPR spectra.

11.4 - Modelling Gd^{3+} electronic relaxation

11.4.1 - Fluctuations of the zero-field splitting term

Fluctuation of the zero-field splitting term has been the subject of numerous studies [Rast *et al.* 2001; Kowalewski and Maler, 2006; Fries and Belorizky, 2007; Helm, 2006]. We previously mentioned that, for an ion like Gd^{3+}, the electrostatic potential of the ligands does not affect the ground term characterised by $L = 0$ to first order of perturbation theory. However, it produces second order effects thanks to the spin-orbit coupling $\lambda \mathbf{L} \cdot \mathbf{S}$, which removes the degeneracy of this term in the absence of an external magnetic field. This removal of the degeneracy which is equal to 8 for Gd^{3+} ($S = 7/2$) is the *Zero-Field Splitting* (ZFS) [Volume 1, sections 6.2 and 8.3.3].

In a molecular reference frame (M) defined by a system of orthogonal axes $\{X, Y, Z\}$ linked to the complex and moving with it, this interaction can be described by a spin Hamiltonian $\hat{H}^{(M)}_{ZFS}(t)$ which depends on the time and generally includes terms of degree $n = 2$, 4 and 6 in $\hat{S}_X, \hat{S}_Y, \hat{S}_Z$. In perturbation theory, these terms involve spin-orbit coupling at increasing degrees and their magnitude decreases rapidly when n increases. We can often limit ourselves to second order terms, except in the case of complexes with cubic or octahedral symmetry for which the mean for this term is null, and for which higher order terms must therefore be considered [Rast *et al*, 2001].

The Hamiltonian $\hat{H}^{(M)}_{ZFS}(t)$ is the sum of its temporal mean $\hat{H}^{(M)}_{ZFS,S}$ and its time-dependent "transient" residual part $\hat{H}^{(M)}_{ZFS,T}(t)$ due to vibrations of the complex and to deformations produced by collisions with neighbouring molecules:

$$\hat{H}^{(M)}_{ZFS}(t) = \hat{H}^{(M)}_{ZFS,S} + \hat{H}^{(M)}_{ZFS,T}(t) \qquad [11.16]$$

The form of the "static" part $\hat{H}^{(M)}_{ZFS,S}$ must respect the mean symmetry of the complex. When the calculation is restricted to second order terms, there is a molecular reference frame $\{X, Y, Z\}$ where this Hamiltonian is written

$$\hat{H}^{(M)}_{ZFS,S} = D_X \hat{S}^2_X + D_Y \hat{S}^2_Y + D_Z \hat{S}^2_Z \qquad [11.17]$$

with $D_X + D_Y + D_Z = 0$. It is convenient to write this term in the following form [Volume 1, section 6.2.2]:

$$\hat{H}^{(M)}_{ZFS,S} = D_S\left[\hat{S}^2_Z - S(S+1)/3\right] + E_S(\hat{S}^2_X - \hat{S}^2_Y) \qquad [11.18]$$

where $D_S = 3D_Z/2$, $E_S = (D_X - D_Y)/2$. To characterise the magnitude of $\hat{H}^{(M)}_{ZFS,S}$, the following parameter can be used

$$\Delta_S = \sqrt{D^2_X + D^2_Y + D^2_Z} = \sqrt{2D^2_S/3 + 2E^2_S} \qquad [11.19]$$

For Gd^{3+} complexes, Δ_S is around 0.05 cm^{-1}, which corresponds to $\Delta_S/\hbar \approx 10^{10}$ rad s^{-1}.

In the laboratory's reference frame (L) identified by the system of orthogonal axes $\{x, y, z\}$, where z is the direction of the field **B**, the total spin Hamiltonian acting on the Gd^{3+} ion is written

$$\hat{H}^{(L)}_{spin}(t) = \hat{H}_{Zeeman} + \hat{H}^{(L)}_{ZFS}(t) \qquad [11.20]$$

The Zeeman term is given by

$$\hat{H}_{Zeeman} = g\beta B\hat{S}_z = \hbar\omega_S\hat{S}_z \qquad [11.21]$$

where ω_S is the resonance angular frequency in the absence of zero-field splitting. $\hat{H}^{(L)}_{ZFS}(t)$ is obtained from $\hat{H}^{(M)}_{ZFS}(t)$ by expressing the components of the spin **S** in the reference frame (M) as a function of its components in the reference frame (L). Due to rotational Brownian motion of the complex, $\hat{H}^{(L)}_{ZFS,S}(t)$ is a random time perturbation, characterised by the rotational correlation time τ_r introduced in section 11.3.2 (equation [11.9]). This perturbation induces transitions between the Zeeman sublevels of the complex, thus contributing to its spin-lattice relaxation. In complement 2 we detail the form of $\hat{H}^{(L)}_{ZFS,S}$ deduced from expression [11.18] through the action of a *rotation R* which transforms the laboratory's reference frame into the molecular reference frame.

It is obviously very complex to rigorously express the transient part of $\hat{H}^{(M)}_{ZFS,T}(t)$ (equation [11.16]). Indeed, deformations of the complex due to collisions, even if they are restricted to the vibrational modes, are difficult to describe mathematically. In addition, this interaction must be expressed in (L) if we wish to determine the random perturbation $\hat{H}^{(L)}_{ZFS,T}(t)$ contributing to the electronic relaxation. We therefore take a very simplified model of $\hat{H}^{(L)}_{ZFS,T}(t)$, assuming that it is produced by a second order Hamiltonian $\hat{H}^{(M)}_{ZFS,T}$ that is *independent of time*, and displays *axial* symmetry in an $\{X', Y', Z'\}$ reference frame linked to the complex:

$$\hat{H}^{(M)}_{ZFS,T} = D_T\left[\hat{S}^2_{Z'} - S(S+1)/3\right] \qquad [11.22]$$

This reference frame is assumed to undergo *pseudo-rotational Brownian motion*, characterised by a correlation time τ_v with the same order of magnitude as the characteristic times of the vibrations and deformations of the complex, i.e., 10^{-12} to 10^{-11} s. τ_v is therefore much shorter than τ_r which is around 10^{-10} to 10^{-8} s (section 11.3.2). It should be noted that the reference frame $\{X', Y', Z'\}$ generally differs from $\{X, Y, Z\}$ in which the static contribution $\hat{H}^{(M)}_{ZFS,S}$ takes the simplified form given in [11.18]. The magnitude of $\hat{H}^{(M)}_{ZFS,T}(t)$, given by the expression $\Delta_T = \sqrt{2D_T^2/3}$ analogous to [11.19], is of the same order as Δ_S. The form of $\hat{H}^{(L)}_{ZFS,T}(t)$ is similar to that of $\hat{H}^{(L)}_{ZFS,S}(t)$ (complement 2).

11.4.2 - Expression for the electronic relaxation time T_{1e} for Gd^{3+}

The electronic relaxation time T_{1e} is the result of random fluctuations of the Hamiltonian

$$\hat{H}^{(L)}_{ZFS}(t) = \hat{H}^{(L)}_{ZFS,S}(t) + \hat{H}^{(L)}_{ZFS,T}(t) \qquad [11.23]$$

where fluctuations of $\hat{H}^{(L)}_{ZFS,S}(t)$ and $\hat{H}^{(L)}_{ZFS,T}(t)$ are characterised by the correlation time τ_r and τ_v, respectively, with $\tau_v \ll \tau_r$. It is difficult to obtain a closed form expression of the relaxation time T_{1e} for the Gd^{3+} ion due to the effect of the Hamiltonian [11.23]. Redfield's theory, based on second order perturbation theory, is much too complicated to be presented here. To be valid, on principle, the two conditions: (1) $\Delta_S\tau_r/\hbar \ll 1$ and (2) $\Delta_T\tau_v/\hbar \ll 1$ must be simultaneously satisfied, which is rarely the case. Indeed, most Gd^{3+} complexes – particularly the bulkiest ones – are characterised by slow reorientation movements such that $\tau_r > 0.1$ ns. Thus, condition (1) is not satisfied, even if condition (2) generally is. The values of T_{1e} calculated by applying Redfield's theory are therefore expected to be false, and indeed this has been demonstrated at low-field [Fries and Belorizky, 2007; Bonnet *et al.*, 2008]. However, unexpectedly, we have demonstrated theoretically and verified by numerical simulation (see section 11.6.2) that this approximation provides a good description of longitudinal electronic relaxation of the Gd^{3+} ion at intermediate MRI fields and higher magnetic fields: the electronic magnetisation M_z tends towards its equilibrium value M_{eq} according to a mono-exponentiel law characterised by a time T_{1e}, with

$$\frac{1}{T_{1e}} = \frac{1}{T_{1e,S}} + \frac{1}{T_{1e,T}} \qquad [11.24]$$

where the contributions from $\hat{H}^{(L)}_{ZFS,S}(t)$ and $\hat{H}^{(L)}_{ZFS,T}(t)$ are given by the expressions obtained by McLachlan from the Redfield approximation [Fries and Belorizky, 2007; McLachlan, 1964]:

$$\frac{1}{T_{1e,S}} = \frac{1}{25}[4S(S+1)-3]\left(\frac{\Delta_S}{\hbar}\right)^2 \tau_r \left(\frac{1}{1+\omega_S^2\tau_r^2} + \frac{4}{1+4\omega_S^2\tau_r^2}\right) \qquad [11.25]$$

$$\frac{1}{T_{1e,T}} = \frac{1}{25}[4S(S+1)-3]\left(\frac{\Delta_T}{\hbar}\right)^2 \tau_v \left(\frac{1}{1+\omega_S^2\tau_v^2} + \frac{4}{1+4\omega_S^2\tau_v^2}\right) \qquad [11.26]$$

The angular frequency ω_S is defined by equation [11.21]. Since $\tau_r \gg \tau_v$, $1/T_{1e,S}$ is much greater than $1/T_{1e,T}$ for $\omega_S = 0$, thus at zero field. But when B and thus ω_S increase, $1/T_{1e,S}$ decreases much faster than $1/T_{1e,T}$. The simulations described in section 11.6.2 show that at low-field ($B < 0.1$ T), electronic relaxation is mainly due to $\hat{H}^{(L)}_{ZFS,S}(t)$, even when the Redfield approximation does not apply, such that [11.25] does not apply. In contrast, $1/T_{1e,T}$ by far exceeds $1/T_{1e,S}$ at intermediate magnetic fields used in imaging ($0.5 \leq B \leq 1.5$ T) [Bonnet *et al.*, 2010].

11.5 - Estimation of the parameters determining the paramagnetic relaxation of protons

11.5.1 - Survey of parameters

To determine the paramagnetic relaxation rate $R_{1,p}$ (equation [11.4]) or in an equivalent manner, the relaxivity r_1 (equation [11.5]), we should know the following:

- ▹ from equations [11.6] to [11.8]: the solvation number q, the Gd-proton r_{GdH} distance, the residence time τ_m for a water molecule in the inner sphere of the complex, and the rotational correlation time τ_r for the complex,
- ▹ according to equations [11.10] to [11.13]: the minimal approach distance b between a proton from a water molecule and the Gd^{3+} ion in the complex, and the translational correlation time $\tau_D = b^2/D$.
- ▹ finally, T_{1e} must be calculated, which requires Δ_S, Δ_T and τ_v in addition to τ_r to be determined according equations [11.24] to [11.26]

Adjustable parameters are often used to interpret relaxivity experiments. This easy solution should be avoided, and the maximum number of parameters should be independently determined using methods that we will present briefly.

- ▹ Several methods can be used to determine the number q of water molecules coordinating Gd^{3+}. For example, it is possible to use variations in the NMR frequency for ^{17}O nuclei in water molecules induced by LnL complexes (L = ligand), where Ln^{3+} is a cation close to Gd^{3+} but for which the electronic relaxation is very fast, e.g. Dy^{3+}. These variations, known as induced paramagnetic shifts, which are independent of the nature of the ligands, are proportional to the solvation number q and the complex concentration. They can therefore be used to measure q [Alpoim *et al.*, 1992]. EuL or TbL are similar to GdL and the τ_{H_2O} and τ_{D_2O} lifetimes for laser-induced luminescence of one of these complexes can be measured in H_2O and D_2O, then the proportionality relation $q \propto \left(\tau_{H_2O}^{-1} - \tau_{D_2O}^{-1}\right)$ [Horrocks and Sudnick, 1979; Parker and Williams, 1996] can be used. The values of q provided by these methods vary between 0 for the Gdttha complex (ttha = triethylenetetraaminehexaacetate) [Chang *et al.*, 1990] and 8 for the aqua-ion $[Gd(H_2O)_8]^{3+}$ [Powell *et al.*, 1996]. However, it should be noted that a Gd^{3+} complex must satisfy $q \leq 2$, for its thermodynamic stability in water to be sufficient to allow its safe use in clinical studies.

- The value of r_{GdH} is very important because of the $1/r^6_{GdH}$ dependence of R_{1m} in equation [11.8]. However, it is often only estimated. With Gd^{3+} poly(amino carboxylate) complexes, a generally accepted reasonable value is $r_{GdH} = 0.31 \pm 0.1$ nm [Caravan, 2009].
- To determine τ_m, the transverse relaxation rate for ^{17}O nuclei of water molecules is measured as a function of temperature, together with variations in their resonance frequency in the presence of Gd^{3+} complexes [Merbach and Toth, 2001].
- The rotational correlation time τ_r for the complex is an essential component of inner sphere relaxivity, but its value is difficult to determine independently. Use of Stokes's rotational diffusion formula [11.9] is limited by the fact that we neither know the effective radius a of the complex, nor the effective rotational viscosity or microviscosity η^r_{mic} of the solution [Rast *et al.*, 2000]. However, the Stokes formula can be used within a family of relatively globular complexes, which have similar chemical structures and hydration properties, and are thus assumed to be subject to the same microviscosity. According to equation [11.9], τ_r is proportional to the volume of the complex. τ_r can be assumed to be proportional to its molecular mass given the relatively constant density of organic matter, such that the values of τ_r for complexes in the family considered vary in proportion to their masses [Aimé *et al.*, 2005]. τ_r can also be estimated by measuring the longitudinal relaxation rate for ^{17}O nuclei from water molecules as a function of temperature [Merbach and Toth, 2001]. Finally, τ_r can be deduced from the longitudinal relaxation times T_1 of deuterium substituted for hydrogen in the L ligand in diamagnetic complexes LaL, YL or LuL, which are analogous to GdL [Merbach and Toth, 2001; Bonnet *et al.*, 2008].
- The *relative diffusion* coefficient D can be estimated by independently measuring the coefficients of self-diffusion of water and of a diamagnetic analogue of GdL: LaL, YL or LuL. These coefficients of self-diffusion can readily be measured by pulsed-magnetic field gradient NMR techniques producing spin echos (of the signal) for protons from diffusing species [Canet *et al.*, 2002; Bonnet *et al.*, 2008].
- Four very important parameters remain: Δ_S, Δ_T and τ_v and b. They can be determined by three methods: (1) measurement of the relaxation time T_1 for water protons as a function of the applied field, and in some cases of the temperature, designated by NMRD (*Nuclear Magnetic Resonance Dispersion*) which involves these four parameters (2) the NMRD for pro-

tons of probe solutes [Bonnet *et al.*, 2010] and (3) analysis of simulated EPR spectra. The two latter techniques only involve Δ_S, Δ_T and τ_v. These three techniques are complementary and they must all be used to verify the coherence of the results. NMRD methods, which have been the subject of numerous studies [Bertini *et al.*, 2001; Kowalevski and Maler, 2006; Helm, 2006; Korb and Bryant, 2005], are beyond the scope of this book.

It should be noted that the correlation times τ_r and τ_v vary strongly with temperature, according to Arrhénius-type laws, with activation energies E_A^r and E_A^v of around 10 kJ mol^{-1} [Merbach and Toth, 2001; Powell *et al.*, 1996].

11.5.2 - What EPR provides

We have seen that the longitudinal electronic relaxation time T_{1e} for the Gd^{3+} ion plays a key role in proton relaxivity, but that it is difficult to measure directly. In contrast, the Δ_S, τ_r , Δ_T, τ_v parameters can be extracted from *simulations of the EPR spectrum* for a liquid solution of complexes, recorded at several temperatures and several frequencies. These parameters can be used to calculate T_{1e}, either by applying equations [11.24] to [11.26], or by the numerical procedure described below in section 11.6. The simulation is made difficult by the complex evolution of the transverse magnetisation of Gd^{3+}, which generally cannot be described by the Redfield approximation based on second order perturbation theory in $\hat{H}_{ZFS}^{(L)}(t)$ and for which the validity conditions detailed in section 11.4.2 must be satisfied [Fries and Belorizky, 2007]. Even when applying this approximation, the evolution is given by a combination of four decreasing exponentials which are tedious to calculate [Rast *et al.*, 2001]. For these reasons, in the following section we present a rigorous method which can be used to simulate both the EPR spectrum and the longitudinal relaxation. This method is conceptually simpler than the Redfield approximation, and it can be readily numerically implemented given the power of modern computers.

EPR can also be used to determine the Landé g factor for the complexed Gd^{3+} ion, which is involved in the expressions [11.8] of R_{1m} and [11.10], [11.11] of R_1^{OS}. However, g is always very close to $g_e = 2.0023$, and this value can be used given the uncertainty of the measurements and the precision of the relaxivity models (at most a few percent).

Experimentally, the EPR spectrum must be recorded over a broad range of frequencies (a few GHz to more than 500 GHz) and temperatures so as to verify

the validity of the structural and dynamic models used in the simulations. The electronic relaxation times for Gd^{3+} complexes in aqueous solution are too short (e.g. $T_{2e} < T_{1e} \cong 10^{-9}$ s for $B = 0.34$ T) to allow free induction decay or echo signals to be observed. We therefore cannot use pulsed techniques, and EPR spectra are therefore recorded using continuous wave spectrometers. This is not without difficulties as the high values of the static and transient zero-field splitting terms, around 0.03 cm^{-1}, and their associated correlation times $\tau_r > 100$ ps and $\tau_v \cong$ a few ps, produce linewidths of several tens of mT at X-band. High concentrations of complexes (1 – 10 mM) are therefore required to obtain a satisfactory signal/noise ratio. The appropriate spectrometers are described in the reference work on the chemistry of contrast agents [Merbach and Toth, 2001].

11.6 - Simulating the EPR spectrum and longitudinal relaxation of gadolinium complexes

11.6.1 - General theory

When a paramagnetic centre of spin S is subjected to a random Hamiltonian $\hat{H}(t)$, the absorption spectrum of the energy of a field $\mathbf{B}_1$ orthogonal to $\mathbf{B} // z$, which oscillates at an angular frequency ω, is given by [Abragam, 1983]:

$$f(\omega) = A \int_0^\infty \cos \omega t \, G_x(t) \, \mathrm{d}t \qquad [11.27]$$

where $G_x(t)$ is the correlation function for the transverse component S_x of the spin:

$$G_x(t) = \langle S_x(t) S_x(0) \rangle = \frac{1}{2S+1} \overline{\mathrm{Tr}[S_x(t) S_x(0)]} \qquad [11.28]$$

In this expression, $S_x(t)$ is defined by

$$S_x(t) = U(t)^\dagger S_x U(t) \qquad [11.29]$$

where $U(t)$ is the evolution operator of the spin states. It is determined by the spin Hamiltonian $\hat{H}(t)$ through Schrödinger's time-dependent equation

$$\mathrm{i}\hbar \frac{\mathrm{d}U(t)}{\mathrm{d}t} = \hat{H}(t) U(t) \qquad [11.30]$$

with the initial condition $U(0) = 0$. In equation [11.28] the trace Tr is taken for the space of spin states of dimension $2S + 1$ and the bar indicates an *ensemble average* calculated over the different realisations of the random Hamiltonian $\hat{H}(t)$. At the initial time, we can write

$$G_x(0) = \frac{1}{2S+1}\mathrm{Tr}\, S_x^2 = \frac{1}{3}S(S+1) \qquad [11.31]$$

In this general formalism, which is valid whatever the speed of fluctuations of $\hat{H}(t)$, the *transverse* electronic relaxation is described by the time dependence of the correlation function $G_x(t)$. Similarly, the *longitudinal* electronic relaxation is described by the time-dependence of the correlation function $G_z(t)$ of the S_z component defined by

$$G_z(t) = \langle S_z(t)S_z(0)\rangle = \frac{1}{2S+1}\overline{\mathrm{Tr}[S_z(t)S_z(0)]} \qquad [11.32]$$

where $$S_z(t) = U(t)^{\dagger} S_z U(t) \qquad [11.33]$$

and $$G_z(0) = {}^{1}\!/_{3}\ S(S+1) \qquad [11.34]$$

Numerical simulation of $G_z(t)$ can be used to *test the validity of equations* [11.25] and [11.26].

For small-sized complexes which perform rapid Brownian rotation, such as the hydrated Gd^{3+} ion (see section 11.7.1), Redfield's theory can be applied to calculate the $G_x(t)$ and $G_z(t)$ functions [Rast *et al.,* 2000, 2001]. But generally, it is necessary to resort to numerical calculations, which are indeed conceptually simpler.

11.6.2 - Numerical simulation of the electronic relaxation of Gd^{3+} by the Monte Carlo method

Consider a solution of Gd^{3+} complexes. In the laboratory's reference frame (L), the random Hamiltonian $\hat{H}(t)$ for the general theory (equation [11.30]) is $\hat{H}^{(\mathrm{L})}_{spin}(t)$, given by equation [11.20], which is the sum of the Zeeman term (equation [11.21]) and the static and transient zero-field splitting terms (equation [11.23]). Fluctuations of these terms are the result of random and pseudo-rotational reorientations (deformations and vibrations) of the complex. We call *spin system* a specific Gd^{3+} complex with its Hamiltonian $\hat{H}^{(\mathrm{L})}_{spin}(t)$. To numerically simulate the evolution of the correlation functions $G_x(t)$ and $G_z(t)$ defined by equations [11.28] and [11.32], a large number of N_{sys} ($500 \leq N_{sys} \leq 3000$) realisations of the spin system must be generated to represent the various possible dynamic situations with good statistical precision. For each realisation, the molecular reference frames $\{X, Y, Z\}$ and $\{X', Y', Z'\}$ associated with the static and transient zero-field splitting terms will be randomly and independently oriented in (L). The dynamics of the spin state for

a realisation can be calculated for a given duration [0, t_{max}] by decomposing this duration into a large number N of very short steps Δt ($t_{max} = N\,\Delta t$) such that $\hat{H}^{(L)}_{spin}(t)$ can be considered constant and equal to $\hat{H}^{(L)}_{spin}(n\Delta t)$ during the interval $n\Delta t \leq t \leq (n+1)\Delta t$ $(0 \leq n \leq N-1)$. During this interval, equation [11.30] can be immediately integrated:

$$U[(n+1)\Delta t] = \exp\left[-\frac{i\hat{H}^{(L)}_{spin}(n\Delta t)\Delta t}{\hbar}\right]U(n\Delta t) \qquad [11.35]$$

The exponential function is calculated by numerical diagonalisation of $\hat{H}^{(L)}_{spin}(n\Delta t)$, which depends on the adjustable parameters Δ_S, τ_r, Δ_T, τ_v. By successive application of equation [11.35] with increasing n, the evolution operator $U(n\Delta t)$ is calculated step-by-step for each realisation. Practical calculation of $\hat{H}^{(L)}_{spin}(t)$, as defined by [11.23], and the method used to generate the random rotational trajectory of the complex are explained in complement 2. The correlation function $G_x(t)$, which is the arithmetic mean of the traces calculated for the different realisations of the spin system (equation [11.28]), can be used to reproduce the EPR spectrum for any field B with a single set of adjusted parameters (equation [11.27]). The correlation function $G_z(t)$, which is obtained in the same way from the $\mathrm{Tr}[S_z(t)S_z(0)]$ traces, describes the longitudinal relaxation of the complex. At high fields, this function is observed to decrease in a mono-exponential manner, with a characteristic time T_{1e} given with good precision by equations [11.25] and [11.26] obtained in the framework of the Redfield approximation.

11.7 - Examples of simulations of EPR spectra for Gd^{3+} complexes

11.7.1 - The hydrated Gd^{3+} complex

Although not compatible with MRI because of its toxicity, the hydrated complex $[Gd\,(H_2O)_8]^{3+}$ has been used in several studies because it is simple to prepare and its symmetric structure is well known. The Gd^{3+} ion is at the centre of a square-based anti-prism the corners of which are occupied by H_2O ligands (figure 11.2). This figure can be obtained by deformation of a rectangular prism with two opposing square faces: we simply symmetrically pivot these faces by an angle of $\pm\pi/8$ around the axis of the prism passing through the centres of the faces. This complex has D_{4h} group symmetry. EPR spectra were recorded for this complex for various resonance frequencies and temperatures. These spectra were interpreted by assuming the implication of the static and transient zero-field splitting terms.

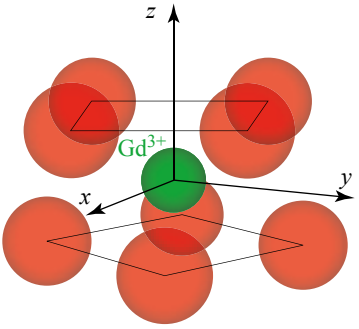

Figure 11.2 - The $[Gd\ (H_2O)_8]^{3+}$ complex. The apexes of the parallel squares are occupied by water molecules.

Figure 11.3 shows representative experimental spectra and their simulations. These were calculated by the Redfield method and validated by Monte Carlo numerical simulation, with the parameters indicated in table 11.2 [Rast *et al.*, 2001]. The parameters were adjusted so as to reproduce a large number of spectra recorded at different frequencies and temperatures, allowing variation of the relative contributions of the static and transient terms to obtain a single set of reasonable values. In particular, we verified that the τ_r value determined complies with Stokes's law [11.9] for a complex with the same size as $[Gd\ (H_2O)_8]^{3+}$ in water.

Table 11.2 - Zero-field splitting parameters and correlation times used to simulate EPR spectra for $[Gd(H_2O)_8]^{3+}$, $[Gd(DOTA)(H_2O)]^{-}$ and GdACX complexes at various frequencies and temperatures. The *g* factors are indicated, as are the activation energies when they were determined.

	$[Gd\ (H_2O)_8]^{3+}$ [a]	$[Gd\ (DOTA)(H_2O)]^{-}$	GdACX
$\Delta_S\ /\hbar\ [10^{10}\ rad\ s^{-1}]$	0.38	0.35	0.45
$\tau_r\ (T_0)\ [10^{-12}\ s]$ [b]	140	491	260
$E^r_A\ [kJ\ mol^{-1}]$	18.9	16.4	
$\Delta_T\ /\hbar\ [10^{10}\ rad\ s^{-1}]$	0.65	0.43	0.34
$\tau_v\ (T_0)\ [10^{-12}\ s]$ [b]	0.63	0.54	8.0
$E^v_A\ [kJ\ mol^{-1}]$	9.2	6.0	
g	1.99273	1.99252	1.985

[a] For simplicity, the amplitudes for static zero-field splitting terms of order 4 and 6, which contribute slightly to electronic relaxation, are not presented [Rast *et al.*, 2001]. [b] T_0 = 298.15 K.

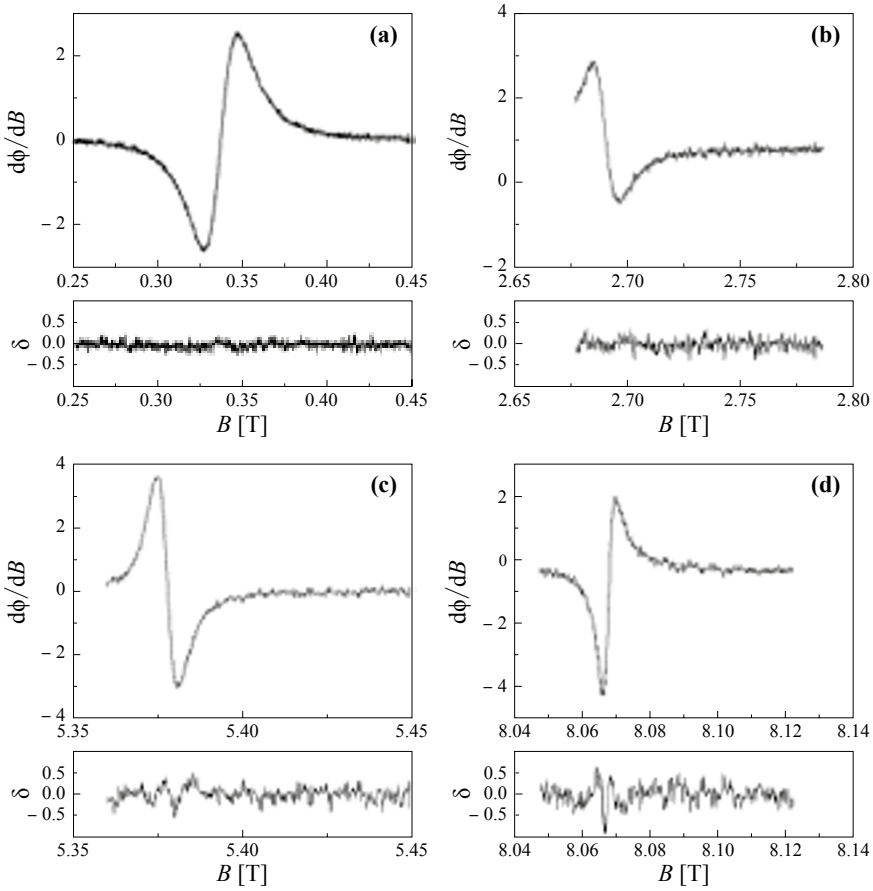

Figure 11.3 - EPR spectra (continuous lines) for the $[Gd(H_2O)_8]^{3+}$ complex recorded at various frequencies and temperatures. **(a)** 9.435 GHz; 354.0 K, **(b)** 75 GHz; 315.1 K, **(c)** 150 GHz; 365.0 K, **(d)** 225 GHZ; 320.1 K. Simulations (dashed lines) were obtained using the parameters listed in table 11.2. The difference Δ between the experimental and calculated spectra is indicated under each spectrum. Note that the experimental spectrum is remarkably well reproduced by the theory. [From Rast S. *et al.* (2001) *J. Am. Chem. Phys.* 123: 2637–2644 © 2001 American Chemical Society, reproduced with permission]

11.7.2 - The GdDOTA complex

To exploit the magnetic properties of the Gd^{3+} ion – which is toxic in its free aqua form – in MRI, it must be sequestered in a multidentate ligand. A multidendate ligand has several electron-donor atoms coordinating the Gd^{3+} ion to form a thermodynamically stable and kinetically inert bio-compatible complex. Polyaminocarboxylates of Gd^{3+} were found to be particularly appropriate, and

several are now used as contrast agents in clinical practice. Here, we will focus on the $[Gd\ (DOTA)(H_2O)]^-$ complex, where DOTA = [1,4,7,10-tetrakis(carboxymethyl)-1,4,7,10-tetra-azacyclo dodecane]. Its structure is shown in figure 11.4.

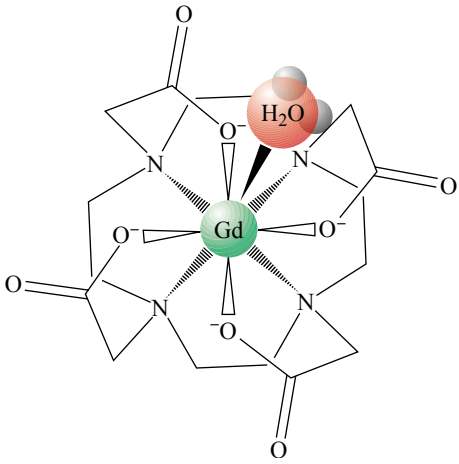

Figure 11.4 - Schematic representation of the structure of the $[Gd\ (DOTA)(H_2O)]^-$ complex.

Its EPR spectrum was simulated at various frequencies and temperatures by applying the Redfield theory and the parameters listed in table 11.2, in line with the Monte Carlo numerical simulation method [Rast *et al.*, 2001]. Figure 11.5 shows a typical X-band EPR spectrum and its simulation.

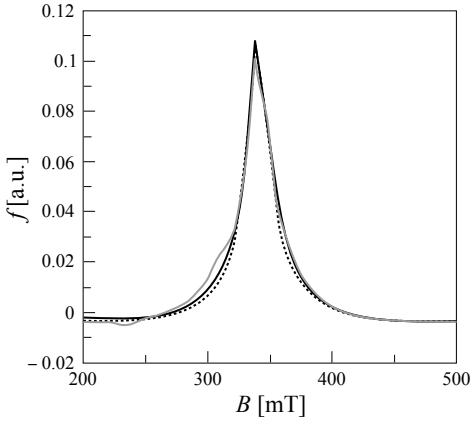

Figure 11.5 - Integrated EPR spectrum for the $[Gd\ (DOTA)(H_2O)]^-$ complex at X-band and T = 274 K. The black line represents the experimental spectrum, the grey line is the simulation given by Redfield's approximation. The dashed line was obtained by the Monte Carlo method. [From Rast S. *et al.* (2001) *J. Chem. Phys.* **115**: 7554–7563

11.7.3 - The GdACX complex

The numerical simulation method described in section 11.6.2 was recently used to reproduce the X-band EPR spectrum for the Gd^{3+}– containing GdACX complex – in which ACX is the cyclodextrine derivative [Bonnet *et al.*, 2008] shown in figure 11.6.

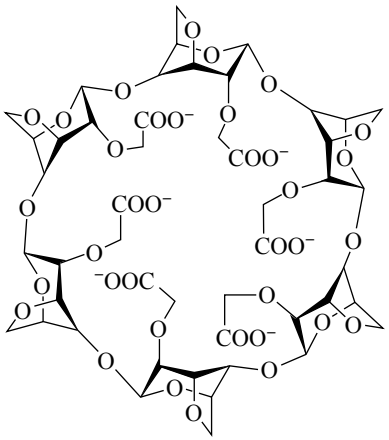

Figure 11.6 - Structure of the ACX^{6-} ligand.

This complex is not stable enough for human injection, but it can be used in animals where it displays acceptable toxicity. It has a high relaxivity due to a strong inner sphere contribution due to the $q = 4$ water molecules coordinating the metal. In animals, it can be used to study models of human brain cancer as, unlike GdDOTA, it remains intra-vascular in the presence of tumour-induced lesions of the hematoencephalic barrier [Lahrech *et al.*, 2008]. This property can be used to quantify the cerebral blood volume, which is an important parameter in tumour vascularisation. Figure 11.7 shows the X-band EPR spectrum for this complex at $T = 298$ K together with simulations by the Redfield method and the Monte Carlo numerical method using the parameters listed in table 11.2.

Note that for all the complexes studied, the values of T_{1e} at the fields used in imaging can be calculated by applying equations [11.24] to [11.26] and the parameters from table 11.2.

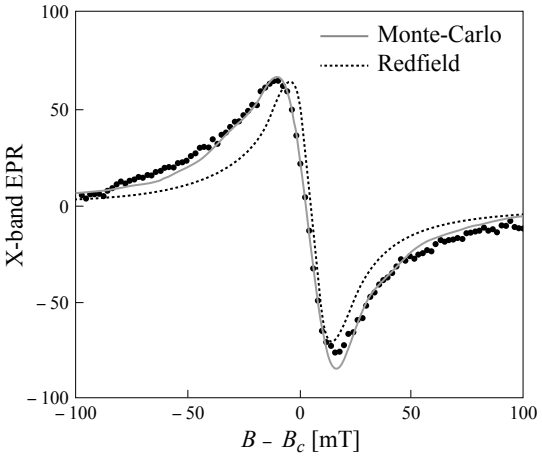

Figure 11.7 - X-band EPR spectrum for the Gd(ACX) complex in aqueous solution at $T = 298$ K. The continuous grey curve is the Monte Carlo simulation, the dashed black line corresponds to the Redfield approximation, which cannot be applied to this slow-rotating bulky complex. B is the applied field, B_c its central value. [From Bonnet C.S. *et al.* (2008) *J. Am. Chem. Phys.* **130**: 10401–10413 © 2008 American Chemical Society, reproduced with permission]

11.8 - Performance of Gd^{3+} complexes as contrast agents

In section 11.3, we described the various molecular parameters of Gd^{3+} complexes which determine the relaxivity of the water protons. Among these, the lifetime τ_m of the water molecules bound to the complex plays an essential role, as indicated by expression [11.6] for R_1^{IS}. A value of $\tau_m = 1/k_{ex}$ shorter than T_{1m} is required in order for exchanges with free water molecules to be as fast as possible and that the free water protons are effectively relaxed by the paramagnetic ions. Numerous derivatives of the basic complexing patterns have been synthesised by chemists, incorporating one or more hydrophobic side-chains likely to increase k_{ex} to more than $10^7\ s^{-1}$, resulting in $\tau_m \leq 100$ ns. The relaxivity r_1 obviously depends on the magnitude B of the applied field and on the temperature. The first GdDOTA contrast agents had relaxivities $r_1 \cong 4$ to $7\ s^{-1}\ mM^{-1}$ at 25 °C in the $B \cong 0.5$ T field, which corresponds to an NMR frequency of 20 MHz. With some recent complexes, a relaxivity of around $50\ s^{-1}\ mM^{-1}$ was obtained in the same conditions.

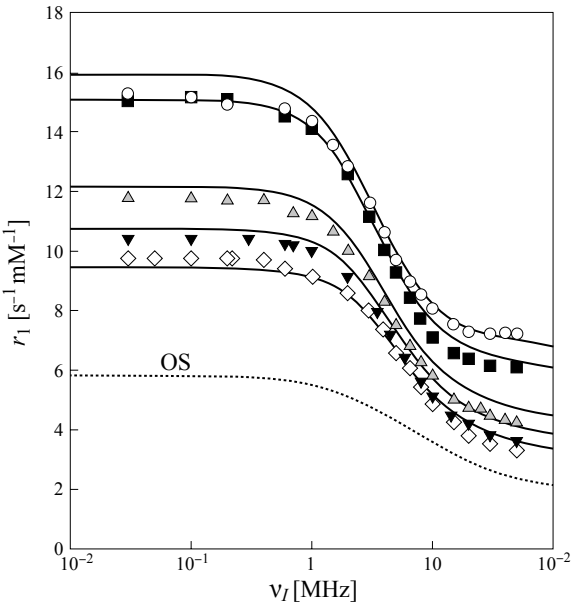

Figure 11.8 - Relaxivity curve $r_1(\nu_I)$ for water protons in a saline solution of [Gd(DOTA)(H_2O)]$^-$ complexes at 277.2 K (white circles), 283.2 K (black squares), 298.2 K (grey triangles), 305.2 K (black triangles), 298.2 K (white diamonds). The continuous theoretical curves were predicted by applying a simplified model limited to the effect of a transient zero-field splitting term (equation [11.22]) to calculate the electronic relaxation. The dashed curve at the bottom of the figure indicates the *outer sphere* contribution to the relaxivity calculated at 298.2 K. [From Powell H., D. *et al.* (1996) *J. Am. Chem. Phys.* **118**: 9333–9346 © 1996 American Chemical Society, reproduced with permission]

In figure 11.8, the relaxivity values $r_1(\nu_I)$ *measured* for the [Gd(DOTA)(H_2O)]$^-$ complex in saline solution are presented as a function of the resonance frequency ν_I of the water protons at various temperatures, along with predictions from a theoretical model [Powell *et al*., 1996]. Figure 11.9 shows the curve for water proton relaxivity induced by the Gd(ACX) complex in a 0.1 M KCl solution at 298 K [Bonnet *et al.*, 2008]. High relaxivity is obtained over a broad frequency range. The calculated curve was obtained using the parameters listed in table 11.2, deduced from simulation of the EPR spectra and other independent measurements. It reproduces the experimental data perfectly.

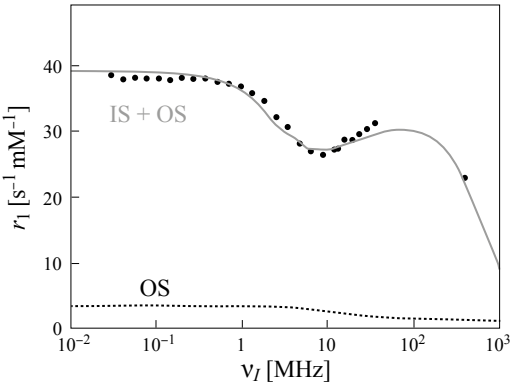

Figure 11.9 - Total relaxivity $r_1(\nu_I)$ (black dots) for water protons in an aqueous solution of Gd(ACX) containing 0.1 M KCl at 298 K. The grey curve is obtained by numerical simulation using the Δ_S, Δ_T, τ_v and g parameters from table 11.2. The value of τ_r was deduced by independent NMR measurements, and the solvation number $q = 4$ was deduced by measuring the lifetime of the luminescence using the method evoked in section 11.5.1. The dashed curve represents the calculated contribution for outer sphere relaxivity. [From Bonnet C.S. *et al.* (2008) *J. Am. Chem. Phys.* **130**: 10401–10413 © 2008 American Chemical Society, reproduced with permission]

Currently, in around 30 % of MRI examinations, radiologists inject Gd^{3+} complexes to improve image contrast and facilitate diagnosis. Figure 11.10 shows the T_1-weighted images of a patient's cerebral tumour before (left) and after (right) injection of the $[Gd(DOTA)(H_2O)]^-$ contrast agent. The contrast agent accelerates the speed of relaxation of the water protons in the tumour which appears as a lighter region, with much better definition, in the right-hand part of the image.

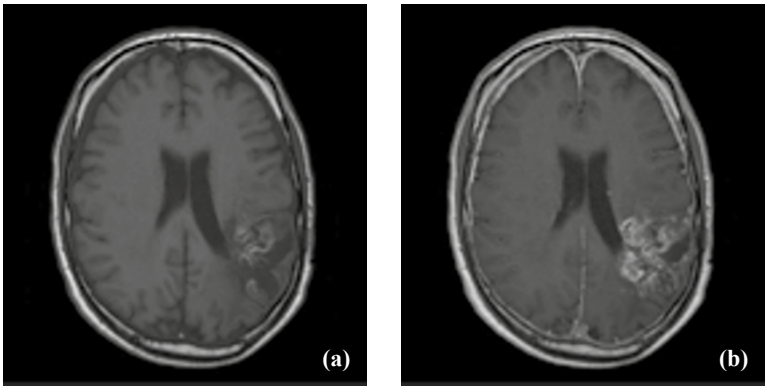

Figure 11.10 - T_1-weighted images acquired at Grenoble University Hospital at 1.5 T, showing a brain tumour **(a)** before and **(b)** after injection of the $[Gd(DOTA)(H_2O)]^-$ contrast agent. The signal for the tumour increases in the presence of the contrast agent – DOTAREM (Guerbet laboratories) – injected at a dose of 0.1 mmol kg^{-1} body weight.

11.9 - Perspectives

Several clues exist to further improve the contrast obtained with Gd^{3+} complexes while maintaining their non-toxicity, which is a pre-requisite for any medical application [Merbach and Toth, 2001; Aimé *et al.*, 2005; Caravan, 2009; De Leon-Rodriguez *et al.*, 2009; Vander Elst *et al.*, 2003; Caravan, 2006; Avedano *et al.*, 2007]. Ligands may be synthesised to produce the highest possible solvation number q compatible with good thermodynamic stability of the complex. Ligands could also be prepared which simultaneously complex several Gd^{3+} ions. Finally, the size of the macromolecular ligand could be increased to enhance the rotational correlation time τ_r, which shortens the longitudinal relaxation time T_{1m} for protons of water molecules coordinating the Gd^{3+} ions at intermediate imaging fields (equation [11.8]) and contributes to increasing R_1^{IS} (equations [11.6] and [11.8]). As mentioned above, the rate of exchange for the water molecules in the first solvation sphere can also be increased, which would reduce the duration of their coordination lifetime τ_m. In summary, the molecular parameters of inner sphere relaxivity must be optimised to satisfy the following conditions:

$$\tau_m < T_{1m} \text{ with } T_{1m} \text{ minimum} \qquad [11.36]$$

Currently, in normal MRI conditions, i.e., at room temperature and fields of 1.5 T, the highest values obtained for r_1 relaxivity are around 50 s^{-1} mM^{-1}.

Several groups recently demonstrated that high relaxivities can be obtained by confining Gd^{3+} complexes in porous hollow nanostructures. Aimé, Sherry and their teams [Aimé *et al.*, 2002; Vasalatiy *et al.*, 2006] observed a considerable increase in the relaxivity of water protons when Gd^{3+} complexes were sequestered in apoferritin nanovesicles. Each nanovesicle has a cavity measuring approximately 7.5 nm in diameter, with pores of 0.3 to 0.4 nm, which are thus permeable to small water molecules but not to bulkier Gd^{3+} complexes. A nanovesicle can contain 6,000 to 8,000 water molecules and around 10 complexes, producing a high local concentration $c \cong 92$ mM. The large relaxivity measured $r_1 \cong 80$ s^{-1} mM^{-1}, can be explained by a rapid exchange between the water molecules inside the nano vesicles and the surrounding water molecules, combined with a strong increase in local viscosity inside the nanovesicles. These effects result in much longer local translational τ_D and rotational τ_r correlation

times than in liquid water which is less viscous at the same temperature [Fries and Belorizky, 2010].

The theory predicts even larger relaxivities for optimised semi-permeable nanovesicles in which Gd^{3+} complexes are sequestered [Fries and Belorizky, 2010]. Finally, we note the very large values of r_1 – up to 100 to 200 s^{-1} mM^{-1} – which were experimentally obtained by sequestering Gd^{3+} complexes in small porous silica particles [Ananta *et al.*, 2010].

Complement 1 - Influence of the rate of exchange of inner sphere water molecules on proton relaxivity

Here, we present a simplified demonstration of expression [11.6] for R_1^{IS}, which was initially obtained by Luz and Meiboom [Luz and Meiboom, 1964]. A more rigorous demonstration, with an extension to three proton sites in chemical exchange, can be found in [Fries and Belorizky, 2010].

We are interested in the longitudinal relaxation rate for protons in water molecules of the solvent which exchange with water molecules coordinated to the complexed Gd^{3+} ions. Thus, the evolution of the component M_f (f for *free*) of their magnetisation along the field **B** towards its equilibrium value $M_{f,eq}$ must be studied. We note M_c (c for *coordinated*) the magnetisation of the protons in water molecules coordinated to the Gd^{3+} ions, and $M_{c,eq}$ its equilibrium value. The orders of magnitude for the two equilibrium magnetisations are very different. Indeed, as the number n_c of protons from the coordinated water molecules is much smaller than the number n_f of protons in free water molecules, we can write:

$$M_{c,eq}/M_{f,eq} = n_c/n_f = P_m \ll 1 \qquad [1]$$

where P_m is the molar fraction of coordinated water molecules.

The magnetisations M_c and M_f vary due to the effect of longitudinal relaxation which already occurs in the absence of chemical exchange. In the presence of exchange and in the absence of a radiofrequency field, the equations describing the evolution of these magnetisations are written:

$$\begin{aligned} \frac{dM_c}{dt} &= -R_{1m}(M_c - M_{c,eq}) - W_{c\to f}\, M_c + W_{f\to c} M_f \\ \frac{dM_f}{dt} &= -R_{1d}(M_f - M_{f,eq}) - W_{f\to c} M_f + W_{c\to f} M_c \end{aligned} \qquad [2]$$

$R_{1m} = 1/T_{1m}$ is the longitudinal relaxation rate for "bound" protons in the absence of exchange, and R_{1d} is the intrinsic relaxation rate for "free" protons. $W_{c\to f}$ and $W_{f\to c}$ are, respectively, the transition probabilities per unit of time from c towards f and from f towards c. $W_{c\to f}$ is none other than the rate constant k_{ex} defined in figure 11.1:

$$W_{c\to f} = k_{ex} = \frac{1}{\tau_m} \qquad [3]$$

where τ_m is the lifetime for an inner sphere water molecule of the complex. The principle of detailed balance leads to the following relation

$$M_{c,eq} W_{c \to f} = M_{f,eq} W_{f \to c} \quad [4]$$

Using equations [1], [3] and [4], we can therefore write

$$W_{f \to c} = \frac{P_m}{\tau_m} \quad [5]$$

We now introduce the *differences* between the magnetisations and their equilibrium values

$$m_c \equiv M_c - M_{c,eq} \; ; \quad m_f \equiv M_f - M_{f,eq} \quad [6]$$

Given [4] and [5], system [2] becomes

$$\begin{aligned} \frac{\mathrm{d}m_c}{\mathrm{d}t} &= -\frac{1}{T_{1m}} m_c - \frac{1}{\tau_m} m_c + \frac{P_m}{\tau_m} m_f \\ \frac{\mathrm{d}m_f}{\mathrm{d}t} &= -R_{1d} m_f - \frac{P_m}{\tau_m} m_f + \frac{1}{\tau_m} m_c \end{aligned} \quad [7]$$

From these coupled equations, we can show that the return of magnetisations M_c and M_f to their equilibrium values is monotonous except during a very short initial period. According to equation [1], we have $|m_c| \ll |m_f|$. Thus, in equations [7], we can neglect $|\mathrm{d}m_c/\mathrm{d}t|$ in comparison with $|\mathrm{d}m_f/\mathrm{d}t|$ after the transient period, i.e., throughout most of the relaxation. With this approximation, the first equation [7] produces the relation

$$m_c \left(\frac{1}{T_{1m}} + \frac{1}{\tau_m} \right) = \frac{P_m}{\tau_m} m_f \quad [8]$$

By substituting m_c into the second equation [7], we obtain:

$$\frac{\mathrm{d}m_f}{\mathrm{d}t} = -R_{1d} m_f - \frac{P_m}{\tau_m} m_f + \frac{P_m}{\tau_m} \frac{T_{1m}}{T_{1m} + \tau_m} m_f = -\left(R_{1d} + \frac{P_m}{T_{1m} + \tau_m} \right) m_f \quad [9]$$

Relaxation of M_f towards its equilibrium value is therefore described by the following equation

$$\frac{\mathrm{d}M_f}{\mathrm{d}t} = -(R_{1d} + R_1^{IS})(M_f - M_{f,eq}) \quad [10]$$

where

$$R_1^{\mathrm{IS}} = \frac{P_m}{T_{1m} + \tau_m} \quad [11]$$

This is equation [11.6] in the main text. This expression shows how the exchange rate of water molecules affects the inner sphere paramagnetic relaxation of protons.

Complement 2 - Elements of the method used to simulate EPR spectra for Gd^{3+} complexes

◇ *Expressions for static and transient zero-field splitting (ZFS) Hamiltonians of Gd^{3+} in the laboratory's reference frame*

In section 11.4.1, we provided the expressions for the "static" $\hat{H}^{(\mathrm{M})}_{\mathrm{ZFS,S}}$ and "transient" $\hat{H}^{(\mathrm{M})}_{\mathrm{ZFS,T}}$ parts of the zero-field splitting Hamiltonian in a *molecular reference frame* (M); we now wish to obtain them in the *laboratory's {x, y, z} reference frame* when we shift from one reference frame to another by *rotation*.

▹ In the molecular reference frame $\{X, Y, Z\}$, the static part is written (equation [11.18]):

$$\hat{H}^{(\mathrm{M})}_{\mathrm{ZFS,S}} = D_{\mathrm{S}}\left[\hat{S}^2_Z - S(S+1)/3\right] + E_{\mathrm{S}}(\hat{S}^2_X - \hat{S}^2_Y) \qquad [1]$$

It is convenient to express $\hat{H}^{(\mathrm{M})}_{\mathrm{ZFS,S}}$ as a function of the standard second order irreducible tensor operators $\hat{T}^q_2$ $(-2 \le q \le 2)$ defined by [Messiah, 2014]:

$$\hat{T}^0_2 = \sqrt{\frac{3}{2}}\left[\hat{S}^2_Z - S(S+1)/3\right],\ \hat{T}^{\pm 1}_2 = \mp\frac{1}{2}(\hat{S}_Z\hat{S}_\pm + \hat{S}_\pm\hat{S}_Z),\ \hat{T}^{\pm 2}_2 = \frac{1}{2}\hat{S}^2_\pm \qquad [2]$$

where $\hat{S}_\pm = \hat{S}_X \pm \mathrm{i}\hat{S}_Y$. We therefore obtain:

$$\hat{H}^{(\mathrm{M})}_{\mathrm{ZFS,S}} = \sqrt{\frac{2}{3}}D_{\mathrm{S}}\hat{T}^0_2 + E_{\mathrm{S}}(\hat{T}^2_2 + \hat{T}^{-2}_2) = \sum_{q=-2}^{2} C^q_2\hat{T}^q_2 \qquad [3]$$

where $C^0_2 = \sqrt{2/3}\,D_{\mathrm{S}}$, $C^{\pm 1}_2 = 0$, $C^{\pm 2}_2 = E_{\mathrm{S}}$.

Now consider a rotation $R(\mathbf{u}, \omega)$ by an angle ω around a unit vector **u**, which transforms the laboratory's $\{x, y, z\}$ reference frame into the $\{X, Y, Z\}$ molecular reference frame. The advantage of irreducible operators is that in this rotation, each operator $\hat{T}^q_2$ becomes $\sum_{q'=-2}^{2} D^2_{q'q}(R)\hat{t}^{q'}_2$, where the $D^2_{q'q}(R)$ quantities are well known elements of the Wigner matrix $D^2(R)$ of dimension 5, and $\hat{t}^{q'}_2$ are the tensor operators [2] expressed using the components $\hat{S}_x, \hat{S}_y, \hat{S}_z$ of **S** in the $\{x, y, z\}$ reference frame [Messiah, 2014]. By replacing the $\hat{T}^q_2$ by their expression as a function of the $\hat{t}^{q'}_2$ in equation [3] we obtain:

$$\hat{H}^{(\mathrm{L})}_{\mathrm{ZFS,S}} = \sum_{q'=-2}^{2} x_{q'}\hat{t}^{q'}_2;\quad x_{q'} = \sum_{q=-2}^{2} D^2_{q'q}(R)\,C^q_2 \qquad [4]$$

▹ The same method can be used to obtain the expression $\hat{H}^{(\mathrm{L})}_{\mathrm{ZFS,T}}$ for the transient part in the $\{x, y, z\}$ reference frame: start with expression [11.22] of $\hat{H}^{(\mathrm{M})}_{\mathrm{ZFS,T}}$ in the molecular reference frame $\{X', Y', Z'\}$, then introduce the

pseudo-rotations $R_T(\mathbf{u}, \omega)$ in place of the overall spatial rotations $R(\mathbf{u}, \omega)$ of the complex.

◇ *Simulation of the random rotational trajectory of a complex*

The calculation of $\hat{H}^{(L)}_{ZFS}$ given by [11.23] requires knowledge of the $D^2_{q'q}(R_t)$ elements of the Wigner matrix, which are used to transform the laboratory's reference frame into the molecular reference frame by applying a random rotation R_t at time t. The rotations R_t defining the random rotational trajectory of the complex, which is assumed to be spherical, are generated by a succession of elementary rotations $R(\mathbf{u}, \Delta\omega)$, where $\Delta\omega$ is a random angle and the direction $\mathbf{u}$ is spatially distributed in an isotropic manner. The distribution of the angles $\Delta\omega$ can be taken to be uniform over a $[-\Delta\omega_{max}, +\Delta\omega_{max}]$ domain, where $\Delta\omega_{max}$ is small. Alternatively, $\Delta\omega$ can randomly take the values $\pm\,\Delta\omega_{max}$. As $R_{t+\Delta t} = R(\mathbf{u}, \Delta\omega)\, R_t$, $R_{n\Delta t}$ is obtained by applying n successive elementary rotations to the initial orientation defined by R_0. For each time step Δt, the angle θ of rotation of an axis linked to the molecular reference frame, for example Z for the real rotation modulating the static part of zero-field splitting, is given by the scalar product $\cos\theta = \mathbf{e}_{t+\Delta t} \cdot \mathbf{e}_t$, where $\mathbf{e}_t$, $\mathbf{e}_{t+\Delta t}$ are the unit vectors along the Z axis at times t and $t + \Delta t$, respectively. The extremity of the $\mathbf{e}$ vector moves with two-dimensional Brownian motion over the unit sphere. According to the Einstein relation, the mean quadratic value of the rotational angle θ is given by

$$\overline{\theta^2} = 4D^r \Delta t \qquad [5]$$

where D^r is the rotational diffusion constant which is linked to the correlation time τ_r introduced in equation [11.9] by the relation $D^r = 1/(6\tau_r)$. The angles $\Delta\omega$ of the random elementary rotations and pseudo-rotations of the complex are chosen such that $\overline{\theta^2}$ is small enough for Δt to be shorter than the relevant correlation time, i.e., τ_r and τ_v for the static and transient parts of the zero-field splitting, respectively. Equation [11.35] can thus be resolved step-by-step to obtain a numerical solution to the evolution equation [11.30] for each realisation of the spin system.

References

Abragam A. (1983) *The Principles of Nuclear Magnetism*, Clarendon Press, Oxford.

Aimé S. *et al*. (2005) *Advances in Inorganic Chemistry* **57**: 173-237.

Aimé S. *et al*. (2002) *Angewandte Chemie International Edition* **41**: 1017-1019.

Alpoim M.C. *et al*. (1992) *Journal of the Chemical Society, Dalton Transaction*: 463-467.

Ananta J.S. *et al.* (2010) *Nature Nanotechnologies* **5**: 815-821.

Avenado S. *et al*. (2007) *Chemical Communications* **45**: 4726-4728.

Ayant Y. *et al*. (1975) *Journal de Physique (Paris)* **36**: 991-1004.

Belorizky E. *et al.* (2008) *Journal of Chemical Physics* **128**: 052315, 1-17.

Bertini I. *et al.* (2001) *Solution NMR of Paramagnetic Molecules*, Elsevier, Amsterdam.

Bonnet C.S. *et al.* (2008) *Journal of the American Chemical Society* **130**: 10401-10413.

Bonnet C.S. *et al.* (2010) *Journal of Physical Chemistry B* **114**: 8770-8781.

Borel A. *et al.* (2002) *Journal of Physical Chemistry A* **106**: 6229-6231.

Borel A. *et al.* (2006) *Journal of Physical Chemistry A* **110**: 12434-12438.

Callaghan P.T. (2003) *Principles of Nuclear Magnetic Resonance Microscopy*, Oxford University Press, New York.

Canet D. (1996) *Nuclear Magnetic Resonance: concepts and methods*, Wiley, New-York.

Caravan P. (2009) *Account of Chemical Research* **42**: 851-862.

Caravan P. (2006) *Chemical Society Review* **35**: 512-523.

Chang C.A. *et al.* (1990) *Inorganic Chemistry* **29**: 4468-4473.

Correas J.M. *et al.* (2009) *Nouvelles recommandations pour l'utilisation des agents de contraste ultrasonores : mise à jour 2008* ; Elsevier Masson SAS: Issy-les-Moulineaux, France.

De Leon-Rodriguez L.M. *et al.* (2009) *Account of Chemical Research* **42**: 948-957.

Fries P.H. & Belorizky E. (2007) *Journal of Chemical Physics* **126**: 204503, 1-13.

Fries P.H. & Belorizky E. (2010) *Journal of Chemical Physics* **133**: 0244504, 1-6.

Fries P.H. & Belorizky E. (2012) *Journal of Chemical Physics* **136**: 074513, 1-10.

Gierer A. & Wirtz K. (1953) *Zeitshrift für Naturforschung A: Physical Science* **8**: 532-538.

Helm L. (2006) *Progress in Nuclear Magnetic Resonance Spectroscopy* **49**: 45-64.

Horrocks W.D. *et al.* (1979) *Journal of the American Chemical Society* **101**: 334-340.

Hwang L.P. & Freed J.H. (1975) *Journal of Chemical Physics* **63**: 4017-4025.

Kiricuta I.C. & Simplaceanu V. (1975) *Cancer Research* **35**: 1164-1167.

Korb J.P. & Bryant R.G. (2005) *Advances in Inorganic Chemistry* **57**: 293-326.

Kowalewski J. & Maler L. (2006) *Nuclear Spin Relaxation in Liquids: Theory, Experiments, and Applications,* Taylor & Francis, Londres.

Lahrech H. *et al.* (2008) *Journal of Cerebral Blood Flow and Metabolism* **28**: 1017-1029.

Ledley R.S. *et al.* (1974) *Science* **186**: 207-212.

Luz Z. & Meiboom S. (1964) *Journal of Chemical Physics* **40**: 2686-2692.

Mansfield P. & Pykett I.L. (1978) *Journal of Magnetic Resonance* **29**: 355-373.

McLachlan A.D. (1964) *Proceedings of the Royal Society of London Series A* **280**: 271-288.

Merbach A.E. & Toth E. (2001) *The Chemistry of Contrast Agents in Medical Magnetic Resonance Imaging*, Wiley, New York.

Messiah A. (2014) *Quantum Mechanics ICS*, Dover Publications, New-York.

Parker D. & Williams J.A.G. (1996) *Journal of the Chemical Society, Dalton Transaction* **18**: 3613-3628.

Powell D.H. *et al*. (1996) *Journal of the American Chemical Society* **118**: 9333-9346.

Rast S. *et al.* (2000) *Journal of Chemical Physics* **113**: 8724-8735.

Rast S. *et al.* (2001) *Journal of the American Chemical Society* **123**: 2637-2644.

Rast S. *et al.* (2001) *Journal of Chemical Physics* **115**: 7554-7563.

Solomon I. (1955) *Physical Review* **99**: 559-565.

Tadamura E. *et al.* (1997) *Journal of Magnetic Resonance Imaging* **7**: 220-225.

Torrey H.C. (1953) *Physical Review* **92**: 962-969.

Vander Elst L. (2003) *European Journal of Inorganic Chemistry* **13**: 2495-2501.

Vasalatiy O. *et al.* (2006) *Contrast Media Molecular Imaging* **1**: 10-14.

Vigouroux C. *et al.* (1999) *The European Physical Journal D* **5**: 243-255.

Volume 1: Bertrand P. (2020) *Electron Paramagnetic Resonance Spectroscopy - Fundamentals*, Springer, Heidelberg.

Vymazal J. *et al.* (1999) *Radiology* **211**: 489-495.

Yazyev O.V. & Helm L. (2008) *European Journal of Inorganic Chemistry* **2**: 201-211.